Supporting Information for

Mono-Dispersed MnO Nanoparticles in Graphene-Interconnected N-Doped 3D Carbon Framework as Highly efficient Gas Cathode in Li-CO_2 Batteries

Siwu Li,‡ Yuan Liu,‡ Junwen Zhou,* Shanshan Hong, Yu Dong, Jiaming Wang, Xing Gao, Pengfei Qi, Yuzhen Han and Bo Wang*

Beijing Key Laboratory of Photoelectronic/Electrophotonic Conversion Materials, Key Laboratory of Cluster Science, Ministry of Education, School of Chemistry and Chemical Engineering, Beijing Institute of Technology
Beijing 100081, P. R. China
E-mail: bowang@bit.edu.cn frostfire@sina.com

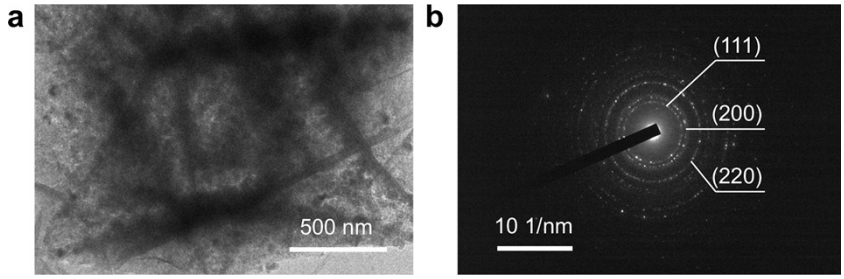

Fig. S1 (a) TEM image of MnO@NC-G and (b) the corresponding SAED pattern.

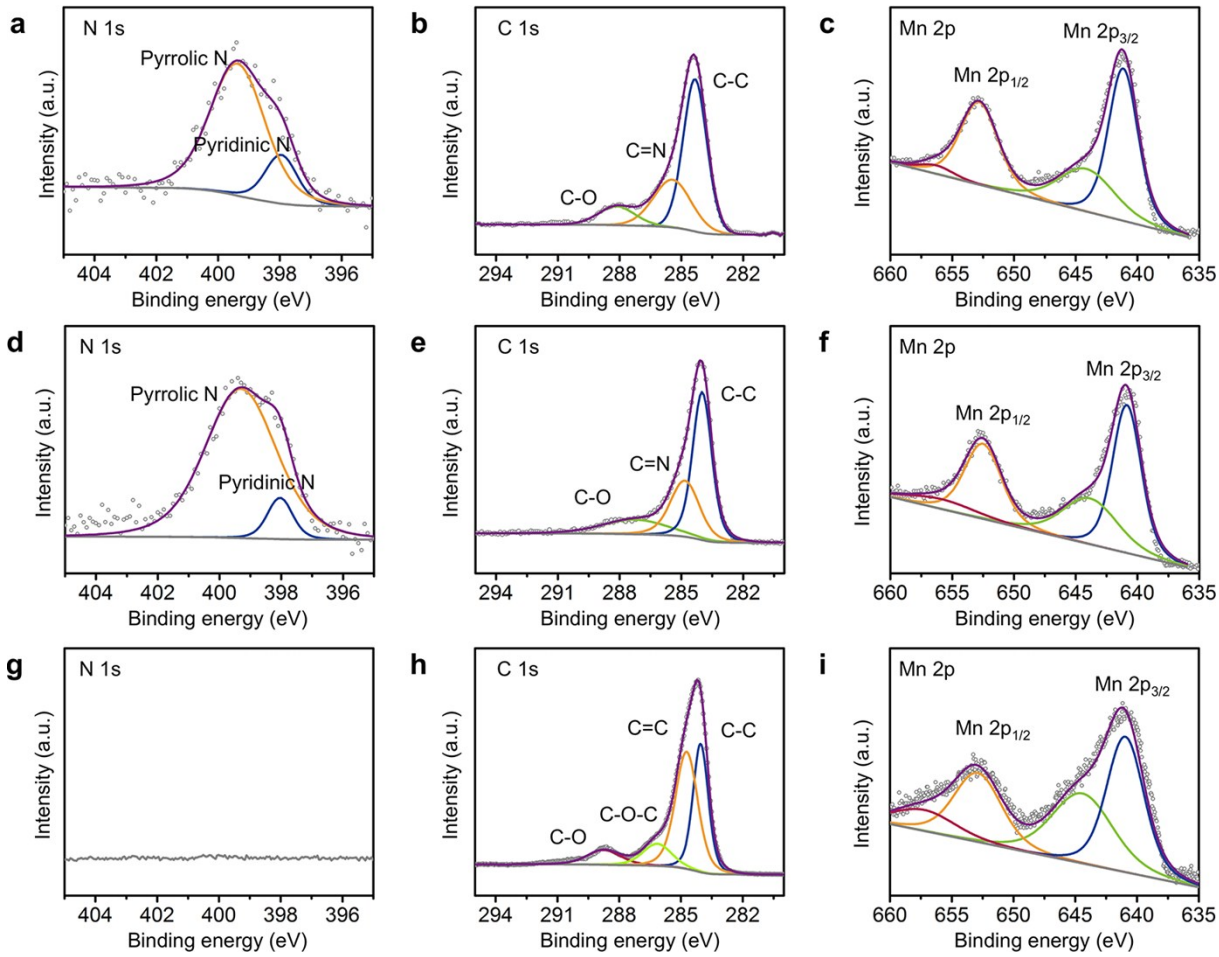

Fig. S2 XPS analysis of (a) – (c) MnO@NC-G, (d) – (f) MnO@NC and (g) – (i) MnO@KB.

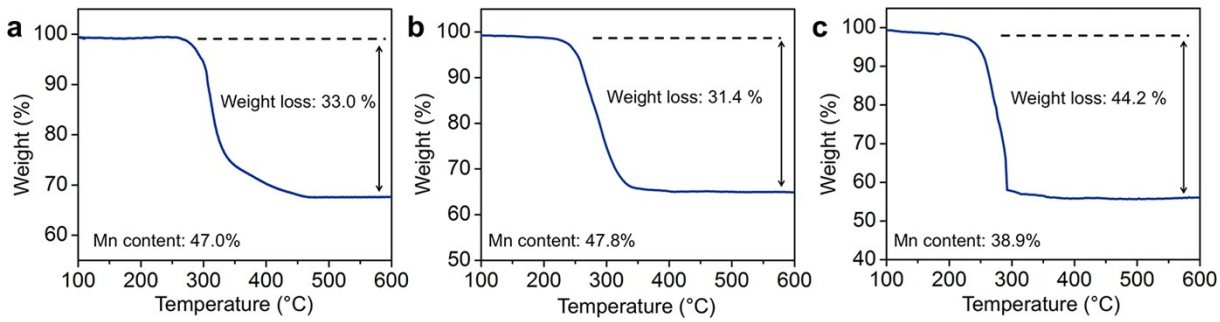

Fig. S3 TG curves of (a) MnO@NC-G, (b) MnO@NC and (c) MnO@KB tested under air atmosphere with a heating rate of 10 °C min^{-1}.

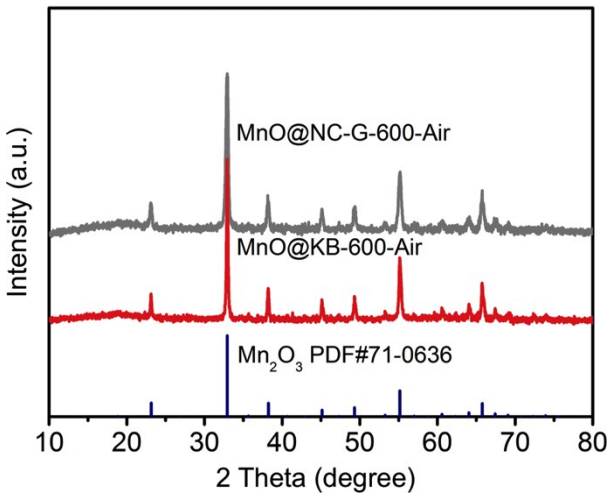

Fig. S4 PXRD patterns of the samples after TG test.

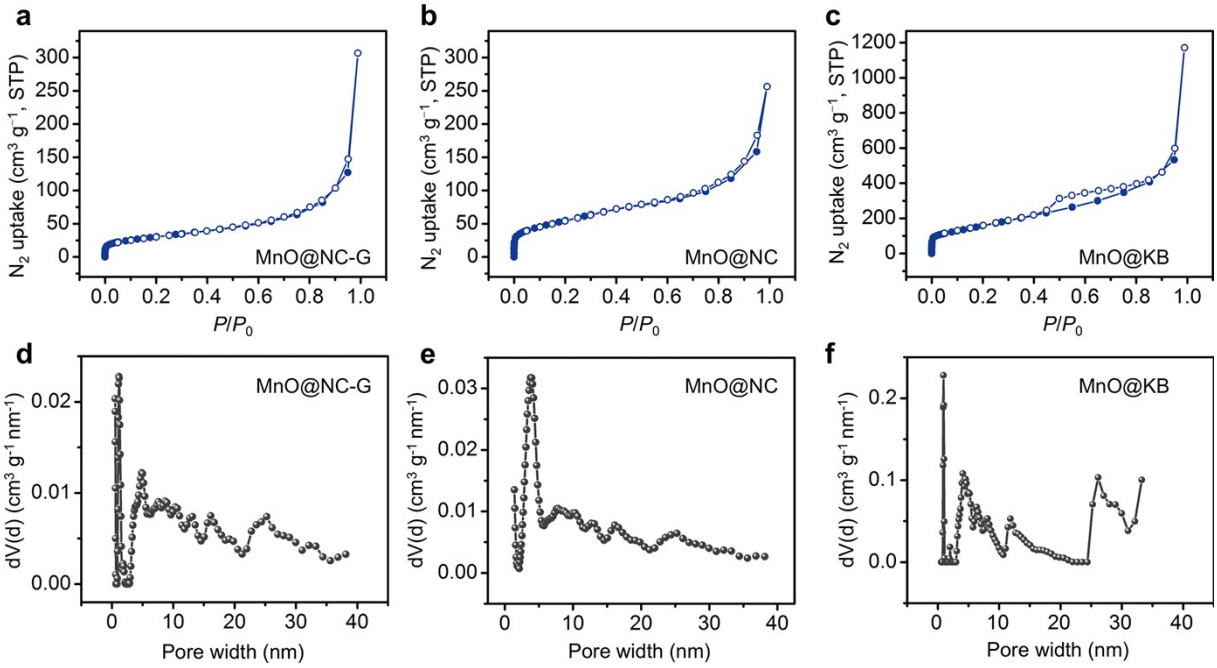

Fig. S5 N_2 adsorption isotherms of (a) MnO@NC-G, (b) MnO@NC and (c) MnO@KB at 77 K and their corresponding pore distributions (d), (e) and (f), respectively.

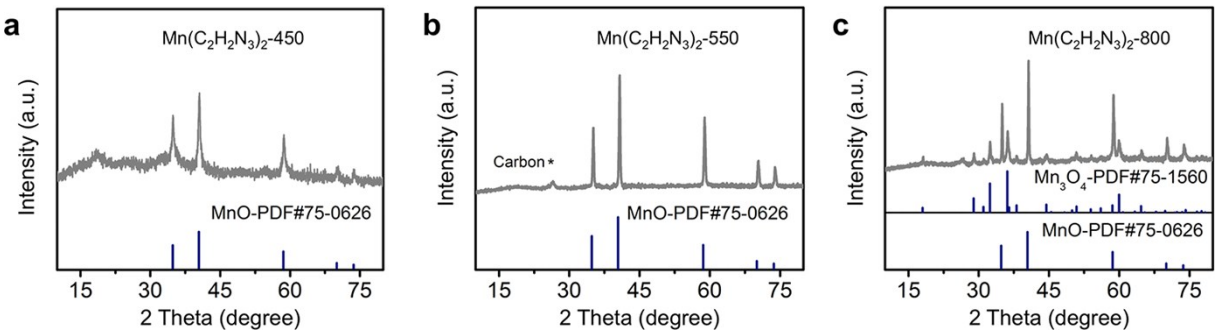

Fig. S6 PXRD patterns of $Mn(C_2H_2N_3)_2$ calcined at (a) 450 °C, (a) 550 °C and (b) 800 °C.

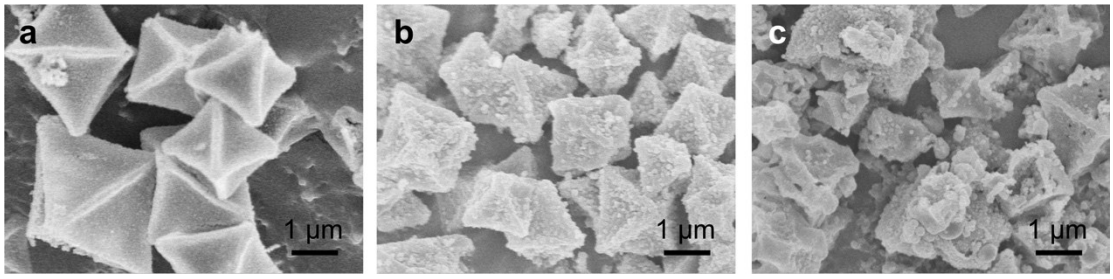

Fig. S7 SEM images of $Mn(C_2H_2N_3)_2$ calcined at (a) 450 °C, (b) 550 °C and (c) 800 °C.

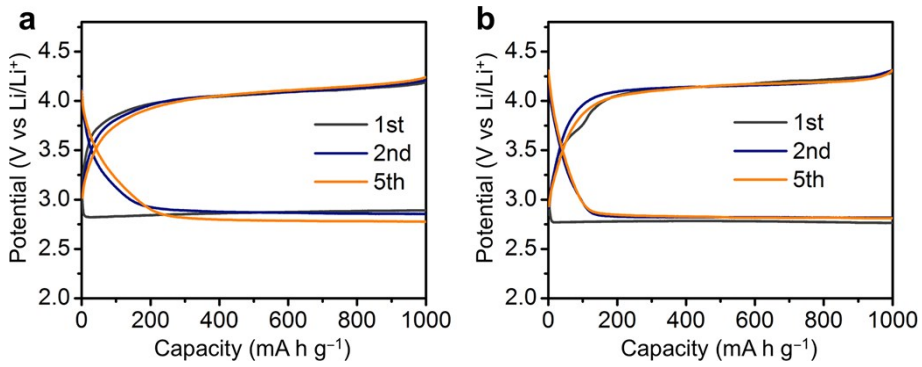

Fig. S8 Discharge-charge cycling performance of (a) MnO@NC-550 and (b) MnO@NC-800 at 100 mA g^{-1}.

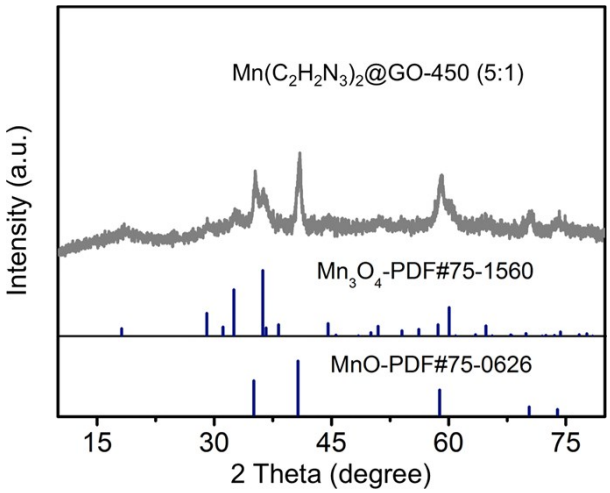

Fig. S9 PXRD patterns of $Mn(C_2H_2N_3)_2$@GO (MOF:GO = 5:1 wt/wt) calcined under 450 °C.

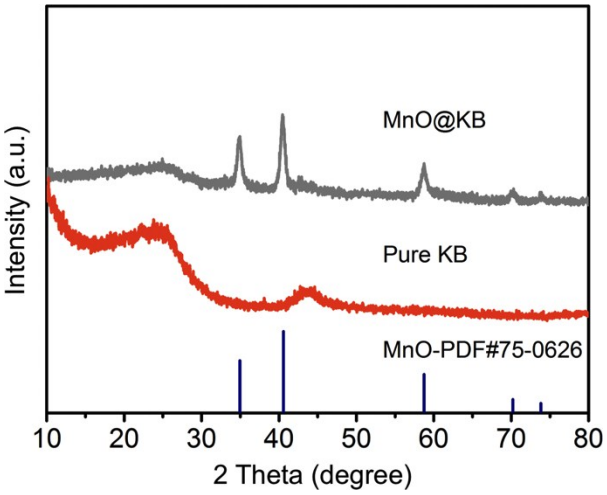

Fig. S10 PXRD patterns of KB and MnO@KB.

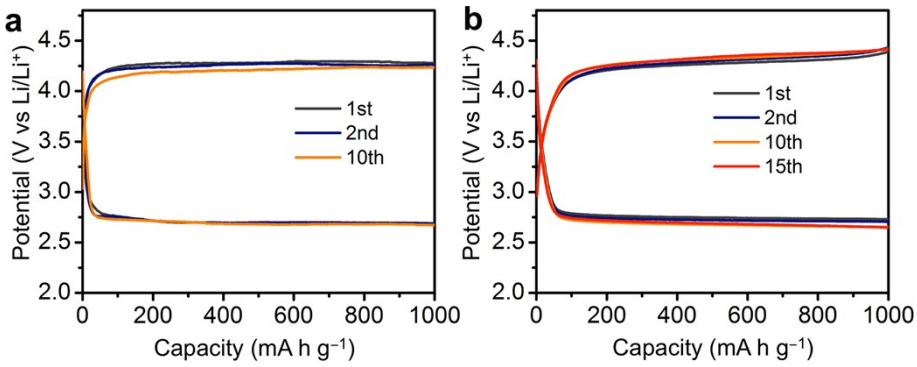

Fig. S11 Discharge-charge cycling performance of $Mn(C_2H_2N_3)_2$ at (a) 50 mA g^{-1}, (b) 100 mA g^{-1}.

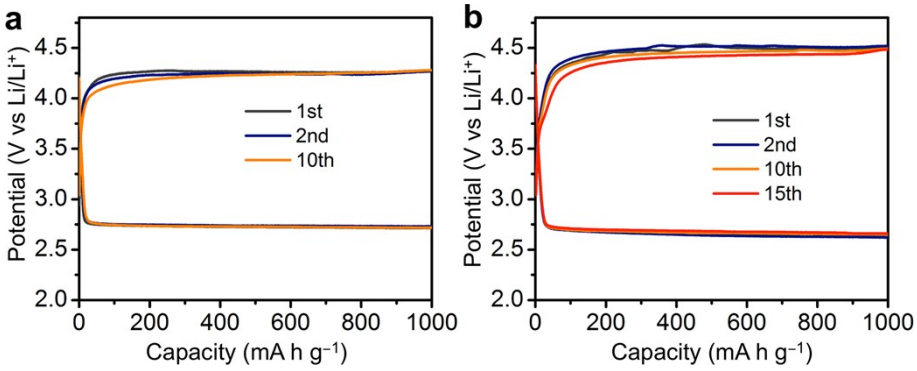

Fig. S12 Discharge-charge cycling performance of bulk MnO at (a) 50 mA g^{-1}, (b) 100 mA g^{-1}.

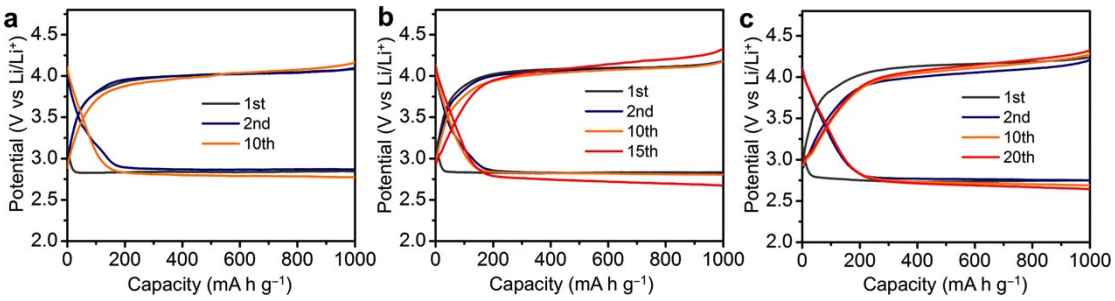

Fig. S13 Discharge-charge cycling performance of MnO@KB at (a) 50 mA g^{-1}, (b) 100 mA g^{-1}, and (c) 200 mA g^{-1}.

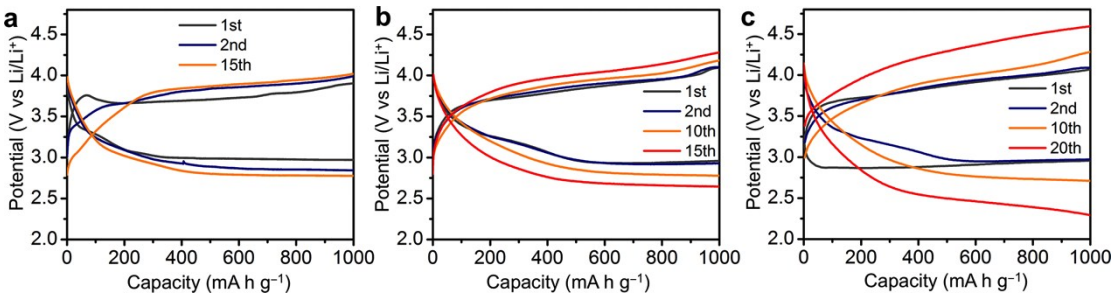

Fig. S14 Discharge-charge cycling performance of MnO@NC at (a) 50 mA g^{-1}, (b) 100 mA g^{-1}, and (c) 200 mA g^{-1}.

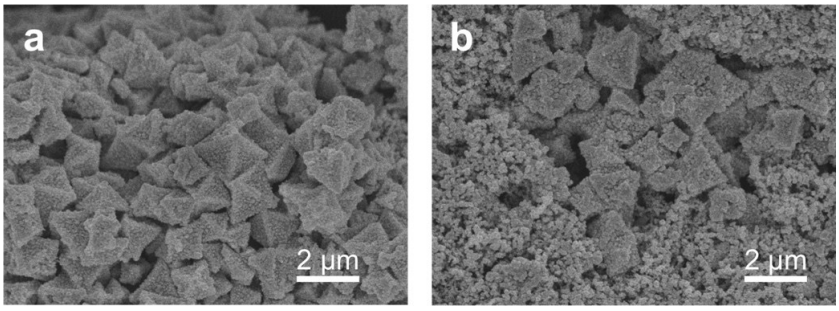

Fig. S15 SEM images of (a) a fresh and (b) a recharged MnO@NC cathode tested under 100 mA g^{-1} and 1000 mA h g^{-1} for 15 cycles.

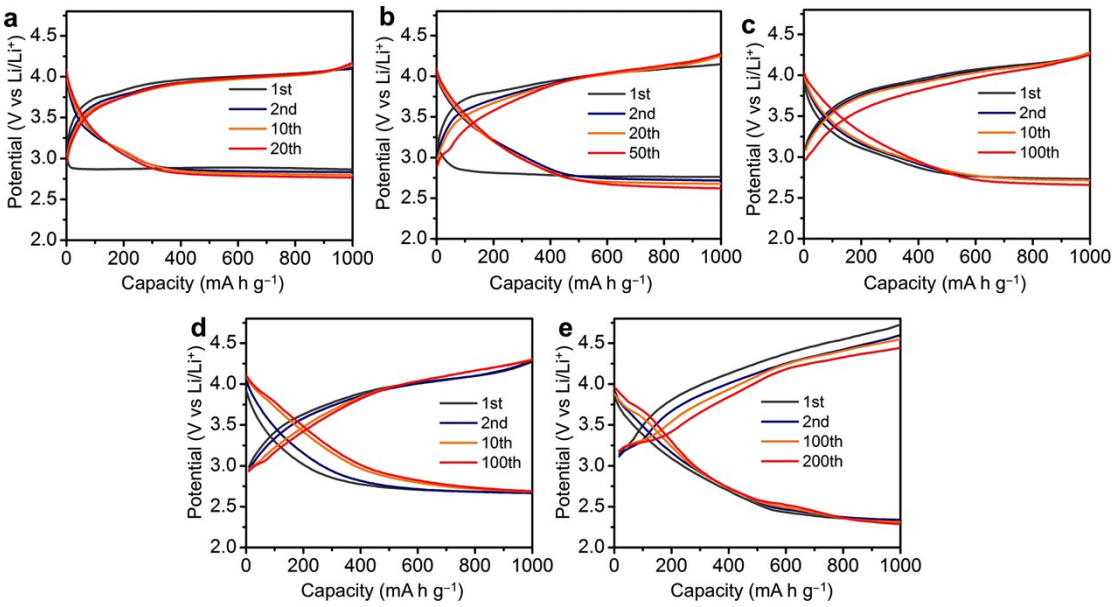

Fig. S16 Discharge-charge cycling performance of MnO@NC-G at (a) 100 mA g^{-1}, (b) 200 mA g^{-1}, (c) 400 mA g^{-1}, (d) 600 mA g^{-1}, and (e) 1000 mA g^{-1}.

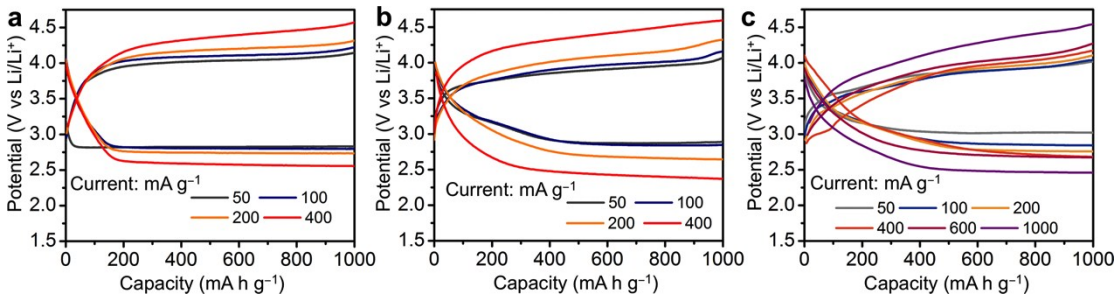

Fig. S17 Rate performance of (a) MnO@KB, (b) MnO@NC and (c) MnO@NC-G cathode.

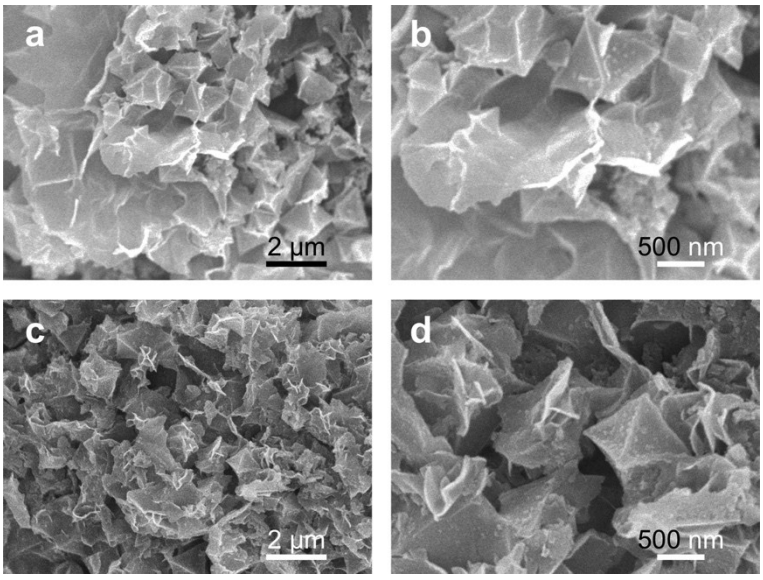

Fig. S18 SEM images of (a, b) a fresh and (c, d) a recharged MnO@NC-G cathode tested under 100 mA g^{-1} and 1000 mA h g^{-1} for 15 cycles.

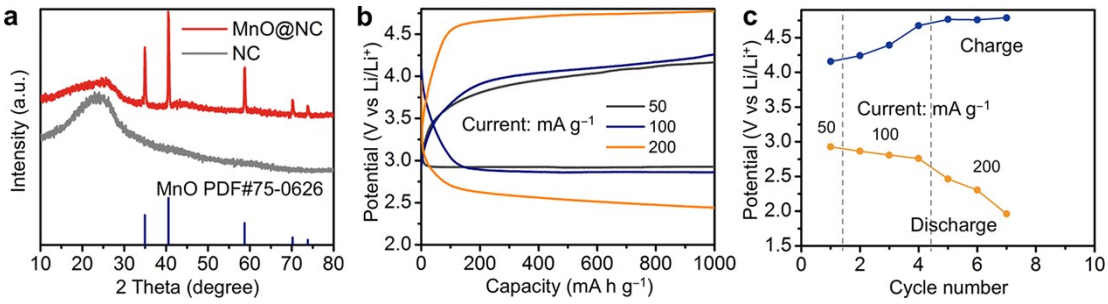

Fig. S19 (a) PXRD patterns of MnO@NC and its derivatives NC. (b) Discharge-charge curves of NC cathodes at different current densities. (c) Rate performance of an NC cathode.

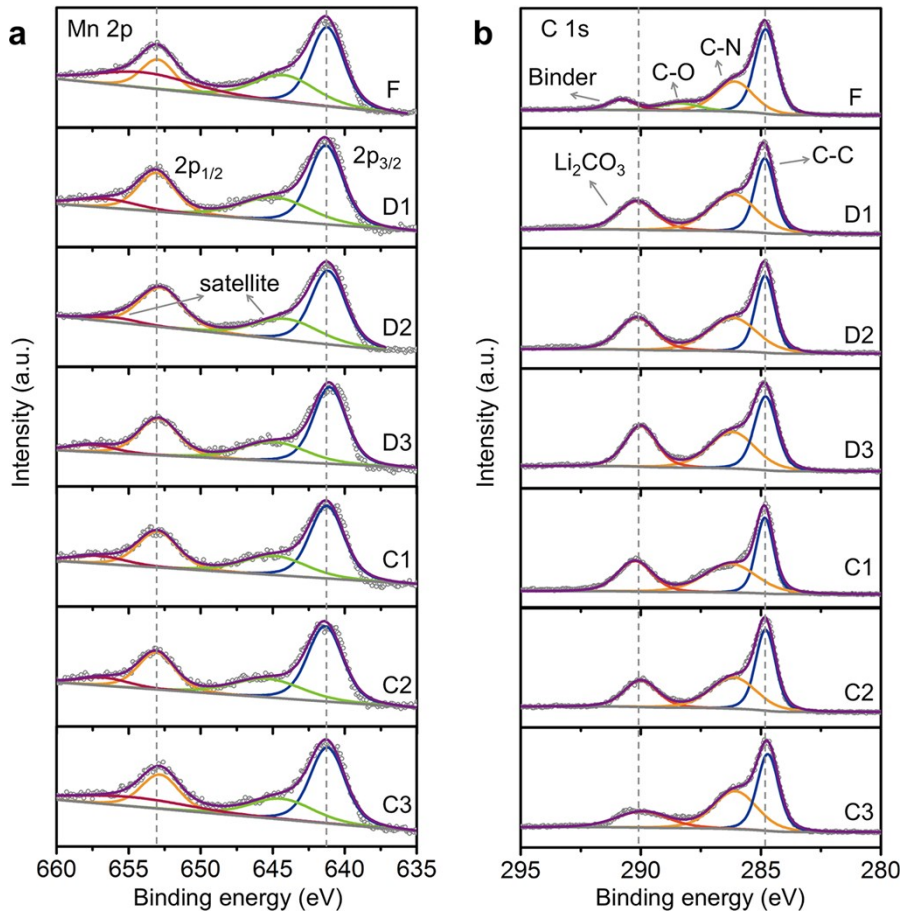

Fig. S20 XPS analysis of MnO@NC-G electrodes at different states during operation at 100 mA g^{-1} (F: fresh electrode; D1-D3: discharge to 200, 500 and 1000 mA h g^{-1}, respectively; C1-C3: recharged to 200, 500 and 1000 mA h g^{-1}, respectively): (a) Mn 2p and (b) C1s spectra.

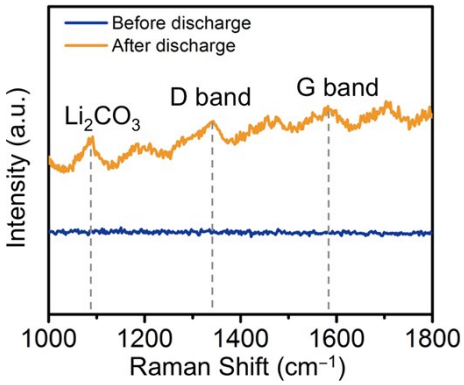

Fig. S21 Raman spectra of Au-coated Ni foam before and after discharge (The electrode was discharged at 100 mA g^{-1} with capacity limit of 1000 mA h g^{-1}).

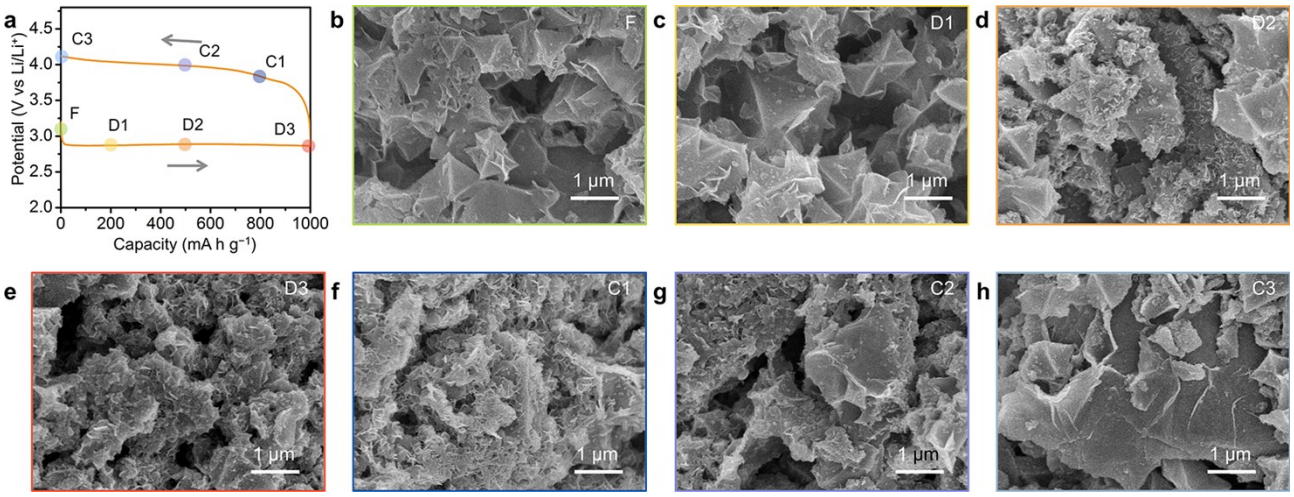

Fig. S22 (a) Discharge-charge voltage curve of MnO@NC-G electrode. (b-h) SEM images of MnO@NC-G electrodes at different states during operation at 100 mA g^{-1} (F: fresh electrode; D1-D3: discharge to 200, 500 and 1000 mA h g^{-1}, respectively; C1-C3: recharged to 200, 500 and 1000 mA h g^{-1}, respectively).

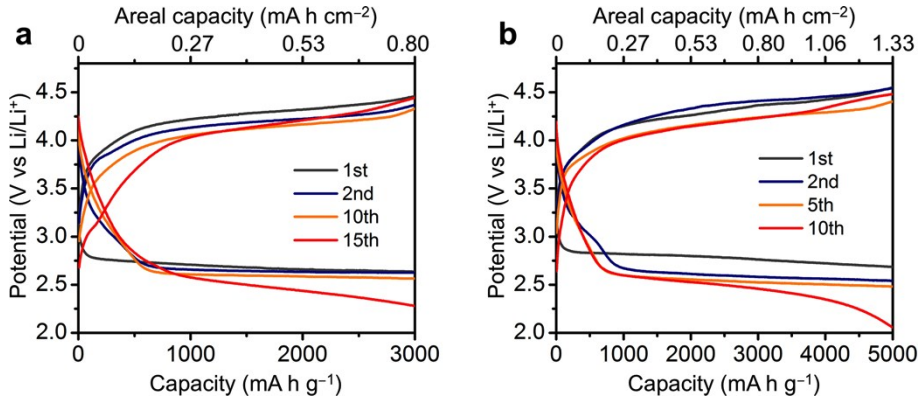

Fig. S23 Discharge-charge cycling performance of MnO@NC-G at 400 mA g^{-1} with a capacity limit of (a) 3000 mA h g^{-1} and (b) 5000 mA h g^{-1}.

Fig. S24 Photographs of (a) a fresh and (b, c) a cycled lithium anode tested under 100 mA g^{-1} and 1000 mA h g^{-1} for (b) 5 and (c) 20 cycles.

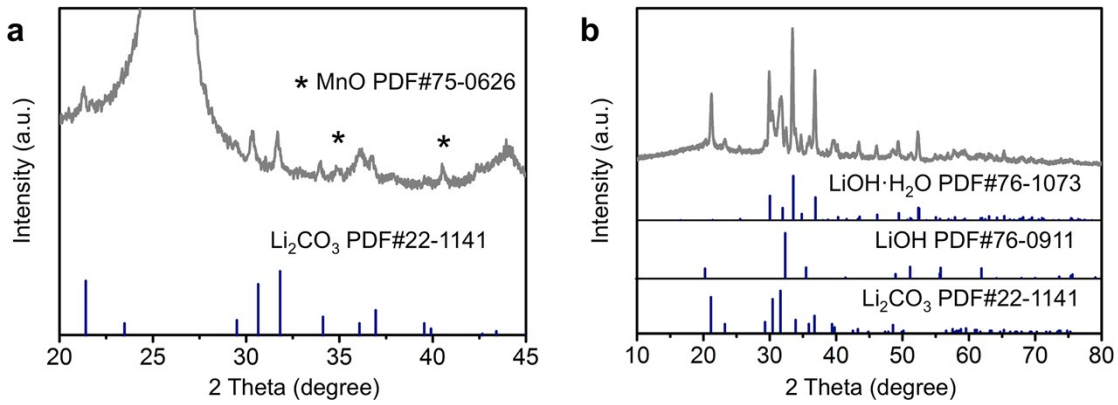

Fig. S25 PXRD patterns of a discharged (a) MnO@NC-G cathode and (b) lithium anode after tested under 100 mA g^{-1} and 1000 mA h g^{-1} for 20 cycles.

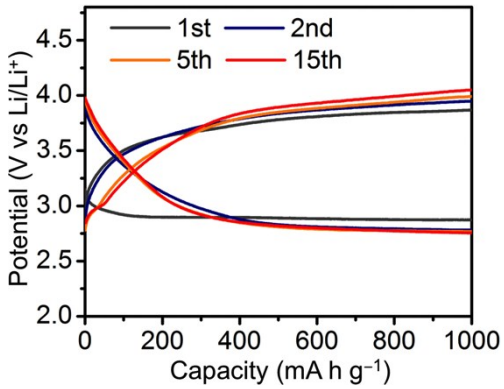

Fig. S26 Discharge-charge cycling performance of a cycled MnO@NC-G cathode under 100 mA g^{-1} and 1000 mA h g^{-1} after replacing the lithium anode and electrolyte.

Table S1. Surface areas and pore volumes of MnO@NC-G, MnO@NC and MnO@KB.

	S_{BET} (m^2 g^{-1})	V_{total} (cm^3 g^{-1})	V_{micro} (cm^3 g^{-1})
MnO@NC-G	110	0.47	0.013
MnO@NC	201	0.40	0.028
MnO@KB	601	1.81	0.038

Table S2. R_s and R_{ct} values of fresh Mn(II) cathodes.

CO_2 electrodes	R_s (Ω)	R_{ct} (Ω)
MnO@NC-G	20	192
MnO@NC	20	205
MnO@KB	22	375
$Mn(C_2H_2N_3)_2$	24	418
Bulk MnO	27	485

Table S3. Summary of the electrochemical performance of reported CO_2 cathodes working in pure CO_2 under similar conditions.

CO_2 cathode	Full discharge capacity (mA h g^{-1})	Voltage hysteresis (V)[a]	Cycle life	Ref.
MnO@NC-G	25021 (50 mA g^{-1})	0.88 (50 mA g^{-1}) 1.18 (100 mA g^{-1}) 1.38 (200 mA g^{-1}) 1.52 (400 mA g^{-1}) 1.58 (600 mA g^{-1}) 1.99 (1000 mA g^{-1})	206 (1 A g^{-1}) 382 (accumulative)	This work
Ketjen Black	1808 (30 mA g^{-1})	1.65 (30 mA g^{-1})	9 (30 mA g^{-1})	1
High surface area carbon	~3000 (0.05 mA cm^{-2})	N/A	N/A	2
CNTs	8379 (50 mA g^{-1}) 5786 (100 mA g^{-1})	1.78 (50 mA g^{-1}) 2.02 (100 mA g^{-1})	29 (50 mA g^{-1})	3
Graphene	14722 (50 mA g^{-1}) 6600 (100 mA g^{-1})	1.50 (50 mA g^{-1}) 1.62 (100 mA g^{-1})	20 (50 mA g^{-1})	4
B,N-codoped holey graphene	16033 (300 mA g^{-1})	1.04 (100 mA g^{-1}) 1.34 (200 mA g^{-1}) 1.56 (400 mA g^{-1}) 1.75 (600 mA g^{-1}) 2.01 (1000 mA g^{-1}) 2.35 (2000 mA g^{-1})	200 (1000 mA g^{-1})	5

Ru@Super P	8229 (100 mA g^{-1})	1.44 (100 mA g^{-1}) 1.65 (200 mA g^{-1}) 1.64 (300 mA g^{-1})	70 (300 mA g^{-1})	6
Mo_2C/CNT[b]	~360 (~5 mA g^{-1})	0.8 (~5 mA g^{-1})	40 (~5 mA g^{-1})	7
Ni-NG	17625 (100 mA g^{-1}) 3900 (200 mA g^{-1})	1.70 (100 mA g^{-1}) 1.93 (200 mA g^{-1})	101 (100 mA g^{-1})	8
NiO-CNT	9000 (100 mA g^{-1})	1.61 (50 mA g^{-1}) 1.97 (100 mA g^{-1})	42 (50 mA g^{-1})	9
Cu-NG	14868 (200 mA g^{-1})	1.14 (200 mA g^{-1}) [c] 1.77 (400 mA g^{-1})	50 (400 mA g^{-1})	10
Ir/C	21528 (50 mA g^{-1})	1.89 (50 mA g^{-1}) 1.62 (100 mA g^{-1}) 1.90 (200 mA g^{-1})	45 (50 mA g^{-1})	11
Mn_2(dobdc)	18022 (50 mA g^{-1})	1.42 (50 mA g^{-1}) 1.44 (100 mA g^{-1}) 1.68 (200 mA g^{-1})	50 (200 mA g^{-1})	12
$Mn(HCOO)_2$	15510 (50 mA g^{-1})	1.56 (50 mA g^{-1}) 1.45 (100 mA g^{-1}) 1.59 (200 mA g^{-1})	50 (200 mA g^{-1})	

[a] The voltage hysteresis value is determined as the gap between the terminal discharge and charge voltages.

[b] Data for Mo_2C@CNT are calculated based on the mass loading of Mo_2C@CNT (3.2 mg) on the cathode. The capacity limit of Mo_2C@CNT is ~30 mA h g^{-1}.

[c] This value is calculated based on the values of the 20th cycle.

References

1. Y. Liu, R. Wang, Y. Lyu, H. Li and L. Chen, *Energy Environ. Sci.*, 2014, **7**, 677-681.
2. S. M. Xu, S. K. Das and L. A. Archer, *Rsc Adv.*, 2013, **3**, 6656-6660.
3. X. Zhang, Q. Zhang, Z. Zhang, Y. Chen, Z. Xie, J. Wei and Z. Zhou, *Chem. Commun.*, 2015, **51**, 14636-14639.
4. Z. Zhang, Q. Zhang, Y. Chen, J. Bao, X. Zhou, Z. Xie, J. Wei and Z. Zhou, *Angew. Chem. Int. Ed.*, 2015, **54**, 6550-6553.
5. L. Qie, Y. Lin, J. W. Connell, J. Xu and L. Dai, *Angew. Chem. Int. Ed.*, 2017, **56**, 1-6.
6. S. Yang, Y. Qiao, P. He, Y. Liu, Z. Cheng, J.-j. Zhu and H. Zhou, *Energy Environ. Sci.*, 2017, **10**, 972-978.
7. Y. Hou, J. Wang, L. Liu, Y. Liu, S. Chou, D. Shi, H. Liu, Y. Wu, W. Zhang and J. Chen, *Adv. Funct. Mater.*, 2017, **27**, 1700564.
8. Z. Zhang, X. G. Wang, X. Zhang, Z. Xie, Y. N. Chen, L. Ma, Z. Peng and Z. Zhou, *Adv. Sci.*, 2018, **5**, 1700567.
9. X. Zhang, C. Y. Wang, H. H. Li, X. G. Wang, Y. N. Chen, Z. J. Xie and Z. Zhou, *J. Mater. Chem. A*, 2018, **6**, 2792-2796.
10. Z. Zhang, Z. W. Zhang, P. F. Liu, Y. P. Xie, K. Z. Cao and Z. Zhou, *J. Mater. Chem. A*, 2018, **6**, 3218-3223.
11. C. Wang, Q. Zhang, X. Zhang, X. G. Wang, Z. Xie and Z. Zhou, *Small*, 2018, **14**, e1800641.
12. S. Li, Y. Dong, J. Zhou, Y. Liu, J. Wang, X. Gao, Y. Han, P. Qi and B. Wang, *Energy Environ. Sci.*, 2018, **11**, 1318-1325.